ISSN 0005-1144
ATKAFF 51(1), 3–18(2010)

Krešimir Vrdoljak, Nedjeljko Perić, Ivan Petrović

Applying Optimal Sliding Mode Based Load-Frequency Control in Power Systems with Controllable Hydro Power Plants

UDK 621.311.07
681.537
IFAC 5.5.4

Original scientific paper

In this paper an optimal load-frequency controller for a nonlinear power system is proposed. The mathematical model of the power system consists of one area with several power plants, a few concentrated loads and a transmission network, along with simplified models of the neighbouring areas. Firstly, a substitute linear model is derived, with its parameters being identified from the responses of the nonlinear model. That model is used for load-frequency control (LFC) algorithm synthesis, which is based on discrete-time sliding mode control. Due to a non-minimum phase behaviour of hydro power plants, full-state feedback sliding mode controller must be used. Therefore, an estimation method based on fast output sampling is proposed for estimating the unmeasured system states and disturbances. Finally, the controller parameters are optimized using a genetic algorithm. Simulation results show that the proposed control algorithm with the proposed estimation technique can be used for LFC in a nonlinear power system.

Key words: Fast output sampling, Genetic algorithm, Identification, Load-frequency control, Power system model, Sliding mode control

Primjena optimalnog kliznog režima upravljanja u sekundarnoj regulaciji frekvencije i djelatne snage razmjene regulacijskim hidroelektranama. U radu se predlaže optimalna regulacija frekvencije i djelatne snage razmjene za nelinearni elektroenergetski sustav. Unutar matematičkog modela sustava jedno se regulacijsko područje sastoji od nekoliko elektrana, manjeg broja koncentriranih trošila i prijenosne mreže. Ostala su regulacijska područja u modelu modelirana pojednostavljeno, nadomjesnim linearnim modelom sustava čiji su parametri dobiveni identifikacijom iz odziva nelinearnog sustava. Taj je linearni model zatim primijenjen u sintezi algoritma sekundarne regulacije koji je zasnovan na kliznom režimu upravljanja. Zbog neminimalno-faznog vladanja hidroelektrana primijenjena je struktura regulatora zasnovana na svim varijablama stanja sustava. Estimacija nemjerljivih stanja i poremećaja zasnovana je na metodi brzog uzorkovanja izlaznih signala sustava. Optimizacija parametara regulatora provedena je korištenjem genetičkog algoritma. Simulacijski rezultati pokazuju kako je predloženi upravljački algoritam, uz predloženu metodu estimacije, moguće koristiti za sekundarnu regulaciju frekvencije i djelatne snage razmjene u nelinearnom elektroenergetskom sustavu.

Ključne riječi: brzo uzorkovanje izlaznog signala, genetički algoritam, identifikacija, sekundarna regulacija frekvencije i djelatne snage razmjene, model elektroenergetskog sustava, klizni režim upravljanja

1 INTRODUCTION

Power systems are complex, nonlinear systems that usually consist of several interconnected subsystems or control areas (CAs). CAs are interconnected by tie-lines. Most of European countries are members of the "European Network of Transmission System Operators for Electricity" (ENTSO-E) interconnection [1].

Deviation of system's frequency from its nominal value is a measure of imbalance between generated and consumed power. When there is more/less generated than consumed active power in a system its frequency increases/decreases. For power system's safe operation it is necessary to keep an equilibrium of consumed and generated active power.

The consumption of electrical energy in a power system constantly changes. Because the electrical energy cannot be stored in sufficient amounts, the task of the power system is to continuously track the amount of consumed power by changing generation of its power plants. That is roughly carried out by day-ahead consumption prediction and most of the power plants in a CA follow their day-ahead hourly schedule. Since the prediction is not perfect, difference of the actual consumption of active power from its predicted value must be compensated by load-frequency

control (LFC). LFC within a CA is in charge of keeping area's frequency at reference value and active power exchanges with all neighbor areas at contracted values. That is obtained by changing reference powers of generators engaged in LFC in a CA. For LFC studies it is usually assumed that each CA consists of a coherent group of generators and that the frequency is unique within each CA. One LFC controller is usually responsible only for its CA.

Before applying any new LFC algorithm to real power system, its behavior must be thoroughly tested through simulations. An example power system is usually modeled as an interconnection of a few CAs. Models for LFC algorithms testing purposes are generally linear and they have all power plants engaged in LFC within a CA replaced with just one substitute power plant [2–5]. That power plant can be of thermal type [6–9] or hydro type [10–13].

Since linearized models are valid only in the vicinity of the operating point, they trustworthily represent real power system dynamics only for close-to-nominal system operation. Changing of power system's operating point is caused by current amount and characteristic of power consumption, characteristics of all power plants within a CA and current number of power plants engaged in LFC in a CA. Additionally, linear models have constant parameters, while parameters of real power systems constantly vary in time, due to their dependency on the operating condition. However, these commonly used models may have nonlinearities within turbines and their governors, but generator dynamics and nonlinearities in tie-lines are usually neglected. Although simplified and linear power system models are mostly used for testing new LFC algorithms, they may not be sufficient to demonstrate algorithm's adequacy and preparedness for proper functioning in real power system.

As opposed, in this paper a detailed nonlinear power system model is used for LFC algorithm testing. In the model one CA is modeled in detail, while other CAs within the interconnection are modeled with several simplifications. Besides, many different nonlinearities are present in the model.

Nowadays, proportional-integral (PI) algorithms with constant parameters are mostly used in real power systems [14–17]. The reasons to replace them with some advanced control algorithm are the following: 1) systems with PI control have long settling time and relatively large overshoots in frequency's transient responses [18]; 2) PI control algorithm provides required behavior only in the vicinity of the nominal operating point for which it is designed; 3) future power systems will rely on large amounts of distributed generation with large percentage of renewable energy based sources and that will further increase system uncertainties [19]; 4) the shortening of time periods in which each level of frequency regulation must be finished is also expected in the future [20].

Therefore, throughout the recent decades many different LFC algorithms were studied [21,22] and they showed very good results on linearized power system models. Those algorithms are based on various methods, such as robust control theory [14, 23], fuzzy logic [12, 24], neural networks [25, 26], model predictive control [27, 28], optimal control [29, 30], adaptive control [31, 32], sliding mode control (SMC) [33, 34] and others. Despite their advantages, new and innovative LFC algorithms have hardly managed to replace classical and proven PI algorithm with constant parameters, which is still prevailing in real power systems.

What is the reason for the prevalent usage of PI algorithm in real power systems despite the development of many advanced control techniques for LFC purpose? Could it be that simplified and linearized models used in the studies of advanced methods are not adequate, and good results obtained on simulations do not replicate in real power systems? In this paper we'll try to find out if that's true by testing the behavior of an advanced LFC algorithm (whose behavior is already proven on linear power system model [35]) on a nonlinear power system model.

The nonlinear model used in this paper is created using MATLAB's SimPowerSystems Toolbox [36]. Although the detailed nonlinear model is used here for testing the algorithm, its synthesis is based on the substitute linearized model, as it is common in control applications. The substitute linear model parameters are obtained by analyzing response signals recorded from the nonlinear model [37].

An advanced controller based on discrete-time SMC from [35] is tested in this paper. When compared to PI controller, this controller shows improvement of system's behavior regarding: better disturbance rejection, maintaining required control quality in the wider operating range, simultaneous shortening of frequency's transient responses and avoidance of the overshoots and also robustness to uncertainties present in the system.

In SMC, system closed-loop behavior is determined by a sub-manifold in the state space, which is called a sliding surface. The goal of the sliding mode control is to drive the system trajectory to reach the sliding surface and then to stay on it. When the trajectory is on the surface, system invariance to particular uncertainties and parameter variations is guaranteed. The trajectory's convergence from any point in state space towards the surface can be ensured with an appropriate choice of a reaching law [38]. The ideal sliding along the sliding surface can only be achieved when continuous-time SMC with very high switching frequency of the control signal is used. Since in real power system LFC control signal is sent to power plants in discrete time, a discrete-time sliding mode controller is used

here. In discrete-time SMC system the trajectory could only be kept inside a small band around the sliding surface. Optimal parameters of the sliding surface and of the reaching law are obtained by an optimization procedure, which is conducted using genetic algorithm (GA).

If only thermal power plants are used for LFC in a CA then stable sliding mode controller can be designed using only measured output signals. But in some power system there are either both, hydro and thermal power plants, or only hydro power plants that are engaged in LFC (e.g. Croatian power system [39]). Sliding mode based on full state feedback must be used in those systems because non-minimum phase behavior is present within a hydro power plant. Therefore, from system's measured output and state, all unmeasured system state must be estimated. State estimation method used here is based on fast output sampling (FOS) [40]. That method is appropriate for estimations in LFC due to the availability of multiple measurements of output signals in each sampling period of the controller. FOS estimation method is also used for the estimation of external disturbance, what additionally improves overall system behavior.

The brief outline of the paper is as follows. Section 2 presents nonlinear power system model and Section 3 describes an identification procedure which results in its substitute linear model. Section 4 describes state and disturbance estimation technique for the substitute model. Section 5 presents discrete-time SMC algorithm, while in Section 6 that algorithm is applied for LFC. Finally, Section 7 contains simulation results obtained on nonlinear power system model.

2 NONLINEAR POWER SYSTEM MODEL

An interconnection of four CAs, as shown in Fig. 1, is used to test the proposed LFC controller. CA1 is modeled in high detail, with many nonlinearities present, while all other CAs are partly simplified. The model is built using SimPowerSystem, which is one of MATLAB's toolboxes. A nonlinear model of CA1 is shown in Fig. 2. CA1 consists of seven power plants, which are hydro power plants (HPPs) or thermal power plants (TPPs). Three hydro power plants (HPPs 1, 2 and 3) are engaged in LFC. All loads within the CA are modeled as three concentrated instances (Loads 1, 2 and 3). Breakers are used to switch parts of loads on or off, or to switch off thermal power plant TPP 2. These switchings are done at different time instances. Transmission lines connecting plants and loads, as well as CAs of the interconnection, are modeled as Π sections of various lengths. Buses are used to measure active powers on important power lines. They measure production of each HPP engaged in LFC and total interchange with neighbor CAs. In each of neighbor CAs total power generation is represented with a single power plant. The power plants in CA3 and CA4 are thermal power plants, while the power plant in CA2 is of hydro type. All values in the model are expressed in per units of their base values, which is common in LFC studies. Although, wherever it is needed, those values are converted into real SI values.

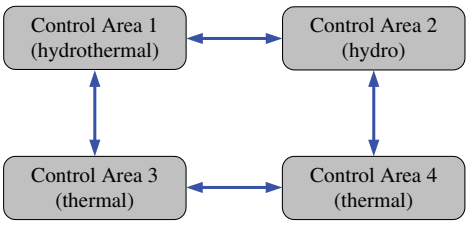

Fig. 1. Four control areas interconnection

There are several inputs to LFC block in Fig. 2: 1) reference value of system's frequency (50 Hz or 1 p.u.), 2) measured value of system's frequency from TPP 1, 3) reference value of total tie line active power, 4) measured value of total tie line active power, and 5) total generated power from all HPPs engaged in LFC. Based on those values, LFC block computes a change in total generation of all power plants engaged in LFC. That generation is then divided among the power plants engaged in LFC and sent to them as control signals u_1, u_2 and u_3.

SMC based LFC algorithm has already been designed for linear power system with hydro power plants engaged in LFC [35]. In order to apply that algorithm to the proposed nonlinear model, a linearization of the nonlinear model must be done firstly.

3 SUBSTITUTE LINEAR POWER SYSTEM MODEL

A linear model of a CA represented with single hydro power plant is shown in Fig. 3, while signals and parameters of that model are given in Tab. 1. The linear model from Fig. 3 can be described with the following equations:

$$\begin{aligned}\dot{\mathbf{x}}_i(t) &= \mathbf{A}_i\mathbf{x}_i(t) + \sum_{\substack{j=1\\ j\neq i}}^{N_{CA}} \mathbf{A}_{ij}\mathbf{x}_j(t) + \mathbf{B}_i\mathbf{u}_i(t) + \mathbf{F}_i\mathbf{d}_i(t),\\ y_i(t) &= \mathbf{C}_i\mathbf{x}_i(t),\end{aligned} \tag{1}$$

where $\mathbf{x}_i \in \mathbb{R}^n$ is the system's state vector, $\mathbf{x}_j \in \mathbb{R}^p$ is a state vector of a neighbor system, $\mathbf{u}_i \in \mathbb{R}^m$ is the control signal vector, $\mathbf{d}_i \in \mathbb{R}^k$ is the disturbance vector and $\mathbf{y} \in \mathbb{R}^l$ is the output vector. Matrices in (1) have appropriate dimensions: $\mathbf{A}_i \in \mathbb{R}^{n\times n}$, $\mathbf{A}_{ij} \in \mathbb{R}^{n\times p}$, $\mathbf{B}_i \in \mathbb{R}^{n\times m}$, $\mathbf{F}_i \in \mathbb{R}^{n\times k}$ and $\mathbf{C}_i \in \mathbb{R}^{l\times n}$. N_{CA} is a number of CAs in the interconnection.

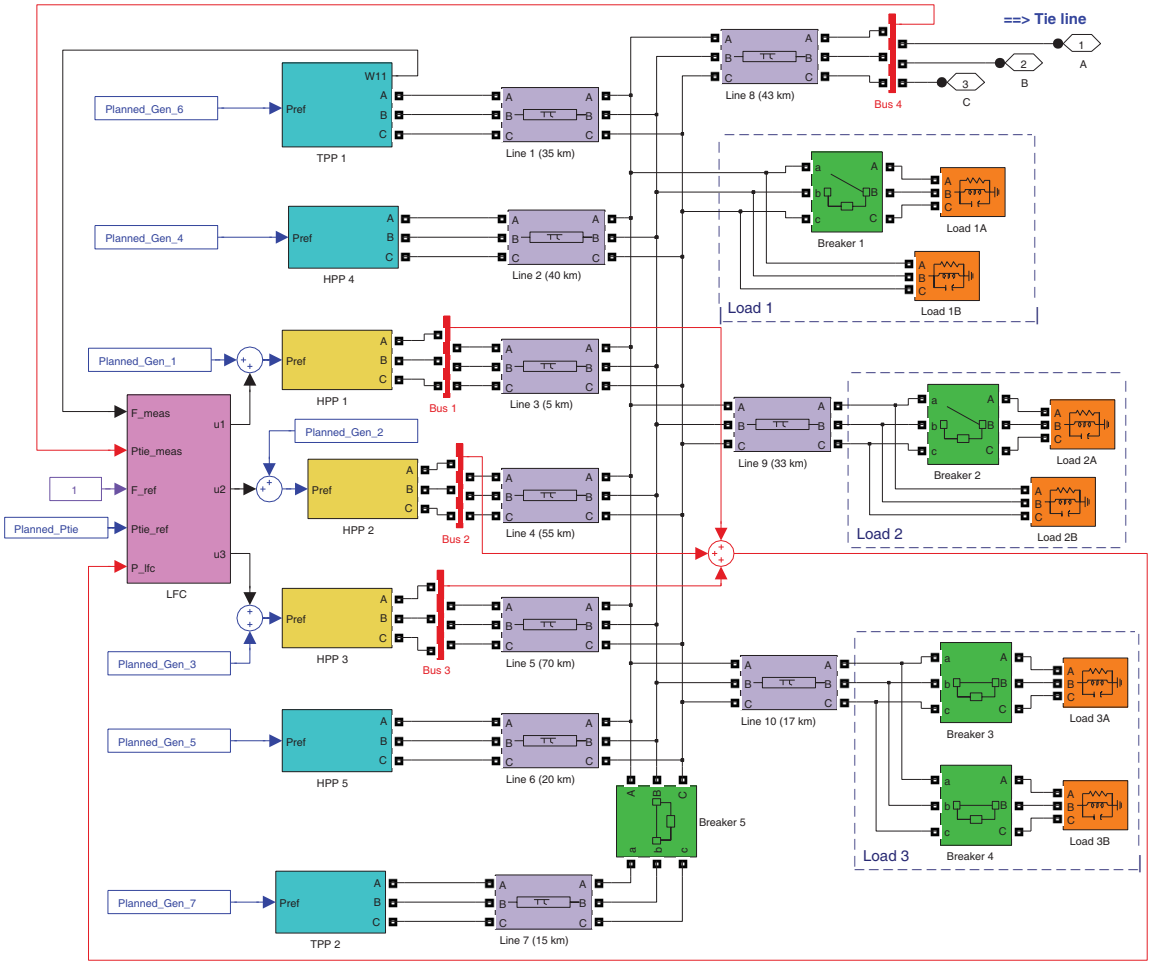

Fig. 2. A nonlinear model of CA1

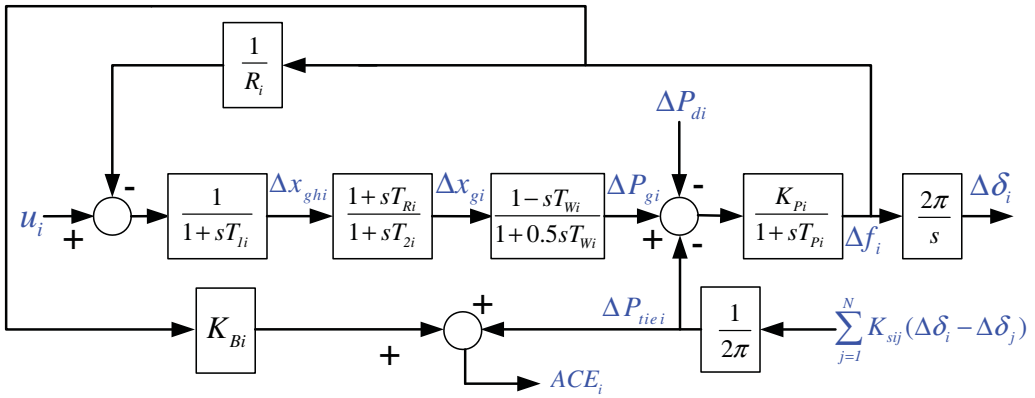

Fig. 3. A linear model of i-th CA represented with hydro power plant

Table 1. Hydro power system variables and parameters

Parameter/variable	Description	Unit
$f(t)$	Frequency	Hz
$P_g(t)$	Generator output power	p.u.MW
$x_g(t)$	Governor valve position	p.u.
$x_{gh}(t)$	Governor valve servomotor position	p.u.
$P_{tie}(t)$	Tie-line active power	p.u.MW
$P_d(t)$	Load disturbance	p.u.MW
$\delta(t)$	Rotor angle	rad
K_P	Power system gain	Hz / p.u.MW
T_P	Power system time constant	s
T_W	Water starting time	s
$T_1,\ T_2,\ T_R$	Hydro governor time constants	s
K_S	Interconnection gain between CAs	p.u.MW
K_B	Frequency bias factor	p.u.MW / Hz
R	Speed droop due to governor action	Hz / p.u.MW
ACE	Area control error	p.u.MW

For the model shown in Fig. 3 state and disturbance vectors from (1) are:

$$\mathbf{x}_i(t) = \begin{bmatrix} \Delta f_i(t) \\ \Delta P_{tiei}(t) \\ \Delta P_{gi}(t) \\ \Delta x_{gi}(t) \\ \Delta x_{ghi}(t) \end{bmatrix}, \qquad \mathbf{d}_i(t) = \Delta P_{di}(t). \tag{2}$$

System matrix from (1) is:

$$\mathbf{A}_i = \begin{bmatrix} -\frac{1}{T_{Pi}} & -\frac{K_{Pi}}{T_{Pi}} & \frac{K_{Pi}}{T_{Pi}} & 0 & 0 \\ \sum_{j=1}^{N_{CA}} K_{Sij} & 0 & 0 & 0 & 0 \\ 2\alpha & 0 & -\frac{2}{T_{Wi}} & 2\gamma & 2\beta \\ -\alpha & 0 & 0 & -\frac{1}{T_{2i}} & -\beta \\ -\frac{1}{T_{1i}R_i} & 0 & 0 & 0 & -\frac{1}{T_{1i}} \end{bmatrix}, \tag{3}$$

and the coefficients in (3) are:

$$\alpha = \frac{T_{Ri}}{T_{1i}T_{2i}R_i},\ \beta = \frac{T_{Ri}-T_{1i}}{T_{1i}T_{2i}},\ \gamma = \frac{T_{2i}+T_{Wi}}{T_{2i}T_{Wi}}. \tag{4}$$

Input and disturbance matrices from (1) are:

$$\mathbf{B}_i = \begin{bmatrix} 0 \\ 0 \\ -2R_i\beta \\ R_i\beta \\ \frac{1}{T_{1i}} \end{bmatrix},\ \mathbf{F}_i = \begin{bmatrix} -\frac{K_{Pi}}{T_{Pi}} \\ 0 \\ 0 \\ 0 \\ 0 \end{bmatrix}. \tag{5}$$

In linearized model of a CA represented with thermal power plant, there are only four states, since there is no state Δx_{gh}, (which is present in hydro CA state vector (2)), due to simpler governor used in thermal power plants. Therefore, matrices $\mathbf{A}_{ij}$ in (1) have dimensions 5×4 or 5×5, depending on whether they are used to describe hydro-thermal (e.g. CA1-CA3 in the interconnection from Fig. 1) or hydro-hydro (e.g. CA1-CA2 in the interconnection from Fig. 1) connection. All elements of matrices $\mathbf{A}_{ij}$ are equal to zero, except the element at position $(1, 2)$, which is equal to $-K_{Sij}$.

The output of the model from Fig. 3 is area control error (ACE) signal. It is introduced as a measure of imbalance between total generated and consumed active power (including power import/export) in each CA. The goal of LFC in each CA is to compensate for ACE deviations. ACE is defined as a combination of frequency deviation in a CA and of total active power flow deviation in tie-lines connecting the CA with its neighbor areas:

$$ACE(t) = K_B\Delta f(t) + \Delta P_{tie}(t). \tag{6}$$

If system output is chosen to be $y_i(t) = ACE_i(t)$, then the system output matrix in (1):

$$\mathbf{C}_i = \begin{bmatrix} K_{Bi} & 1 & 0 & 0 & 0 \end{bmatrix}. \tag{7}$$

Ideally, parameter K_B in (6) should ensure that the value of ACE in a CA is equal to zero when disturbances in other CAs appear, and as close to the negative value of disturbance just after it appears within the CA, before LFC starts to take effect.

Parameters of the substitute linear model can be identified from the responses of the nonlinear model. Since identification procedure presented in [41] can only be used for CAs that have only one power plant engaged in LFC, it

can not be used here because LFC in CA1 from Fig. 2 is conducted using three HPPs. Therefore, different identification method must be used.

3.1 Identification of substitute linear model parameters

In this paper, a procedure based on GA is used for parameters identification. GA is a random search optimization algorithm which is appropriate for finding global optimal solution inside a multidimensional searching space [42].

GA is used here to find an optimal set of linear model parameters for CA1 (Fig. 3), within the interconnection from Fig. 1. That parameter set is defined as:

$$\mathbf{\Theta} = \begin{bmatrix} T_1 & T_2 & T_R & T_W & R & K_P & T_P & K_{S12} & K_{S13} \end{bmatrix}, \tag{8}$$

where K_{S12} and K_{S13} are interconnection gains between CA1 and its neighbor areas, CA2 and CA3, respectively.

The optimal set is the one that minimizes deviation between responses of the linear model and the measured signals from the nonlinear model, when identical control and disturbance signals are applied in both models. For the identification procedure it is essential to firstly bring the system into steady state operating point by using LFC. Then any further LFC action is disabled and small step signals are applied as control and disturbance signals, because linear models are valid only in the vicinity of the operating point.

For identification purposes, the deviation is evaluated by the following fitness function:

$$\Phi_i(\mathbf{\Theta}) = \int_0^{T_s} \left[(f_L(t) - f_N(t))^2 + \rho (P_{gL}(t) - P_{gN}(t))^2 + \right.$$
$$\left. + \varrho (P_{tieL}(t) - P_{tieN}(t))^2 \right] dt, \tag{9}$$

where T_s is identification time horizon, $\mathbf{\Theta}$ is given in (8), ρ and ϱ are weighting factors, while indices L and N denote linear and nonlinear model, respectively.

A detailed flow chart of GA used for parameters identification is shown in Fig. 4. From random initial population GA computes candidate sets of parameters and computes the fitness function of each set based on simulation results. Then it starts a loop of evolution processes, consisting of selection, crossover and mutation, in order to improve the average fitness function of the whole population. Besides the evolved chromosomes, each new generation also includes the best chromosome from the previous generation (elitism) and one random new chromosome. The optimization ends when maximal number of generations is produced. Parameters of the used GA are shown in Tab. 2.

Identification results are shown in Fig. 5. The optimal parameters of the substitute linearized model of CA1 are obtained as: $T_1 = 314.97$ s, $T_2 = 0.92$ s, $T_R = 17.94$ s, $T_W = 0.15$ s, $R = 4.39$ Hz/p.u.MW, $K_P = 5.73$ Hz/p.u.MW, $T_P = 2.65$ s, $K_{S12} = 4.42$ p.u.MW and $K_{S13} = 0.12$ p.u.MW.

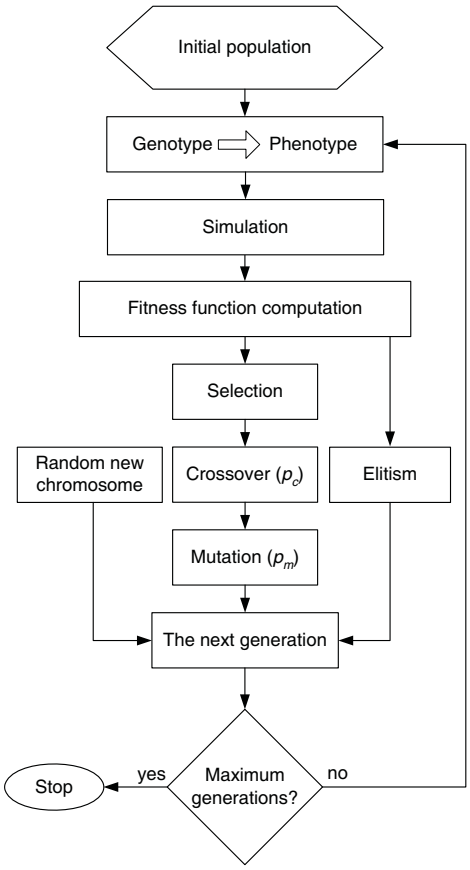

Fig. 4. Flow chart of GA algorithm

Table 2. Parameters of GA used for identification

Parameter	Description	Value
r	Size of population	150
g	Genes per chromosome	9
b	Bits per gene	15
p_c	Probability of crossover	0.7
p_m	Probability of mutation	0.005
N_g	Number of generations	150
ρ	P_g weighting factor	0.1
ϱ	P_{tie} weighting factor	0.05

From Fig. 5 it can be seen that frequencies in both models are practically identical, while there are significant differences in generated power and tie line power deviation signals. The first reason for that is because three power

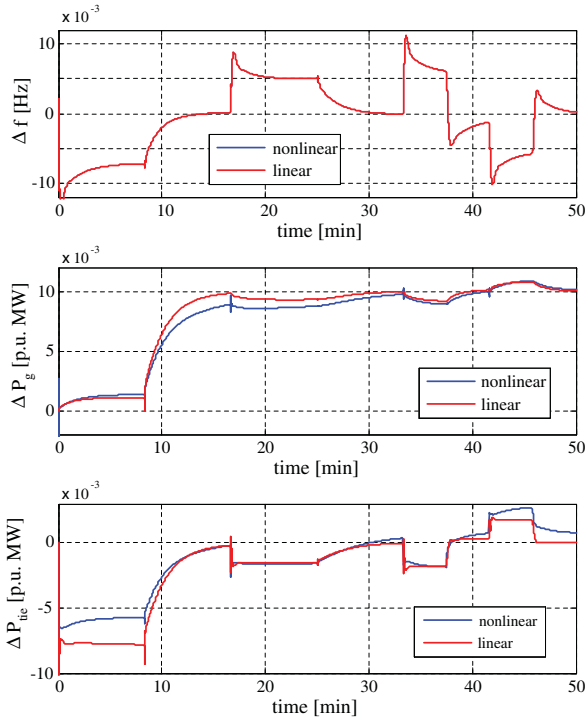

Fig. 5. Comparison between nonlinear and linear model

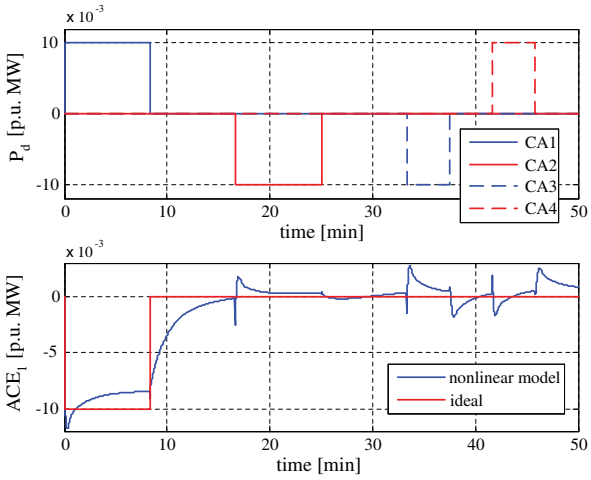

Fig. 6. Ideal and true ACE signals

plants engaged in LFC in the nonlinear model are substituted with just one power plant in the linear model. The second reason is oversimplification of tie line dynamics description in the linear model. Nevertheless, the results are satisfactorily, since robust algorithm will be used for LFC.

Once the identification of the substitute linear model is done, area's state dynamics can be described as:

$$\dot{\mathbf{x}}_i(t) = \mathbf{A}_i\mathbf{x}_i(t) + \sum_{\substack{j=1 \\ j\neq i}}^{N_{CA}} \mathbf{A}_{ij}\mathbf{x}_j(t) + \mathbf{B}_i\mathbf{u}_i(t) + \\ + \mathbf{F}_i\mathbf{d}_i(t) + \boldsymbol{\xi}_i(\mathbf{x},\mathbf{u},t), \tag{10}$$

where $\boldsymbol{\xi}_i$ is a vector of uncertainties. Among other uncertainties, the uncertainty term $\boldsymbol{\xi}_i(\mathbf{x},\mathbf{u},t)$ in (10) includes all linearization errors.

In this paper, the value of parameter K_B from (6) is not found using GA, but it is chosen such that the minimal deviation of steady state ACE signal from its ideal behavior is ensured, as it is shown in Fig. 6. Those results are obtained with LFC turned off. It is impossible to achieve ideal behavior of ACE signal, since that would require K_B to constantly change its value. In fact, in ENTSO-E interconnection K_B is set yearly for each control area and its value is based on portion of area's yearly generation in total yearly generation of the whole interconnection [43]. Nevertheless, with LFC turned on, the difference of K_B's true value from its ideal value is noticeable only during the transient period, since steady state ACE value is independent of the value of K_B.

Additional advantage of the proposed identification procedure is that it could also be used for identifying parameters of substitute linear model representing real power system, since it uses only signals that are commonly measured in real power systems.

Once the substitute linear model is obtained and its parameters found, it can be used for LFC algorithm synthesis. Since most of advanced control algorithms need the knowledge of full system state, to apply one of them for LFC, unmeasured system state of the linear model must be estimated.

4 SYSTEM STATE AND DISTURBANCE ESTIMATION

In real power system the measured signals are: frequency, tie line powers and each plant's generated power, so those signals are considered measurable in both linear and nonlinear model used in this paper. Therefore, signals of governor valve position deviation (Δx_g) and governor valve servomotor position deviation (Δx_{gh}) in the substitute linear model of hydro power plant (Fig. 3) must be estimated. Further improvement in system performance can be achieved if load disturbance (ΔP_d) and the influence of neighbor CAs ($\sum \mathbf{A}_{ij}\mathbf{x}_j$) are also estimated.

To simplify state and disturbance estimation procedures, uncertainties are hereby neglected, and their influence to system behavior is addressed in Section 5.

4.1 State estimation

To estimate unmeasured state of the substitute linear model of CA1, a subsystem shown in Fig. 7 is used.

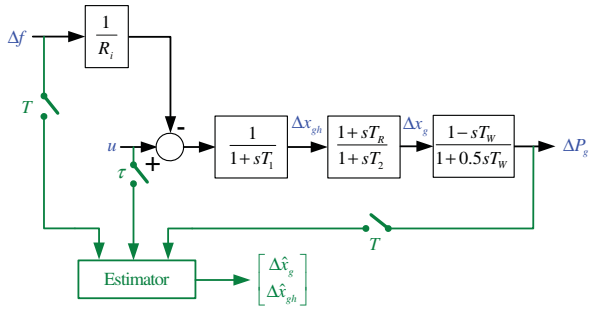

Fig. 7. A dynamical subsystem for state estimation

As it can be seen there are two input signals to the subsystem from Fig. 7: frequency deviation Δf (sampled with period T), and control signal u (sampled with period τ). The sampling periods of input signals are different because in ENTSO-E interconnection control signal u is sent to the power plants every 1-5 seconds [16, 43], while within each period of that signal, there can be multiple measurements of system's frequency f. The subsystem's output signal is total generated output power of all power plants engaged in LFC (it is assumed here that all of them are of hydro type). The output signal can also be measured with the same sampling period as the frequency signal. Since period T is few times smaller than period τ, estimation procedure based on FOS can be used for state estimation [44].

FOS is an estimation technique appropriate for continuous-time systems with discrete-time input signals and where the output signals can be sampled several times during one period of the input signals [40]. Therefore, FOS could be used here for state estimation, but slight modification are needed, due to different sampling periods of two input signals in the subsystem from Fig. 7.

FOS shows better performance than standard estimation techniques, because it reduces the estimation error to zero after just one sampling period [44], while standard estimators need several sampling periods to achieve errorless estimation in high order systems [40].

The principle of using FOS in system's control loop is shown in Fig. 8. Firstly, last N subsamples of the output signal y, measured in the most recent sampling period τ, are used to estimate the system state x. Then, that estimated state is used to compute the control signal u for the next sampling period τ.

For simplicity it is assumed here that it is:

$$T = \frac{\tau}{N}, \tag{11}$$

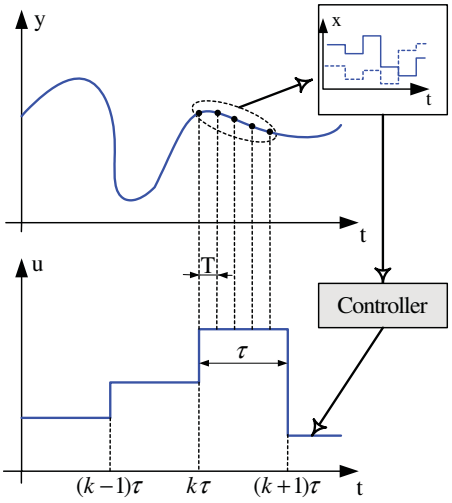

Fig. 8. FOS estimation method in system control

where is $N \in \mathbb{N}$.

To apply FOS, a discrete-time system model must be used. Therefore, the discrete-time approximation of subsystem from Fig. 7, obtained using Zero-Order-Hold (ZOH) discretization method with sampling period T is given as:

$$\begin{aligned} \mathbf{x}_H((k+1)T) &= \mathbf{G}\mathbf{x}_H(kT) + \mathbf{H}(\Delta f(kT) + u(k\tau)), \\ \Delta P_g(kT) &= \mathbf{C}\mathbf{x}_H(kT), \end{aligned} \tag{12}$$

where is $\mathbf{x}_H = \begin{bmatrix} \Delta P_g & \Delta x_g & \Delta x_{gh} \end{bmatrix}^T$.

Values of state variable of subsystem from Fig. 7 in N consecutive subsamples, during constant value of control signal u, can be obtained by iteratively using state equation from (12):

$$\begin{aligned} \mathbf{x}_H(k\tau) &= \mathbf{x}_H(k\tau) \\ \mathbf{x}_H(k\tau + T) &= \mathbf{G}\mathbf{x}_H(k\tau) + \mathbf{H}(\Delta f(k\tau) + u(k\tau)), \\ \mathbf{x}_H(k\tau + 2T) &= \mathbf{G}^2\mathbf{x}_H(k\tau) + (\mathbf{G}\mathbf{H} + \mathbf{H})u(k\tau) + \\ &\quad + \mathbf{G}\mathbf{H}\Delta f(k\tau) + \mathbf{H}\Delta f(k\tau + T), \\ &\vdots \\ \mathbf{x}_H(k\tau + (N-1)T) &= \mathbf{G}^{N-1}\mathbf{x}_H(k\tau) + \sum_{i=0}^{N-2}(\mathbf{G}^i\mathbf{H})u(k\tau) + \\ &\quad + \sum_{i=0}^{N-2}\mathbf{G}^i\mathbf{H}\Delta f(k\tau + (N-2-i)T). \end{aligned} \tag{13}$$

From (12) and (13) it follows that N consecutive subsamples of output signal ΔP_g, measured during constant

value of control signal u, can be computed as:

$$\mathbf{P}^*_{\mathbf{g}k} = \tilde{\mathbf{G}}\mathbf{x}_H(k\tau) + \tilde{\mathbf{H}}u(k\tau) + \mathbf{Q}\mathbf{f}^*_k, \tag{14}$$

where are:

$$\mathbf{P}^*_{\mathbf{g}k} = \begin{bmatrix} \Delta P_g(k\tau) \\ \Delta P_g(k\tau+T) \\ \Delta P_g(k\tau+2T) \\ \vdots \\ \Delta P_g(k\tau+(N-2)T) \\ \Delta P_g(k\tau+(N-1)T) \end{bmatrix}, \ \tilde{\mathbf{G}} = \begin{bmatrix} \mathbf{C} \\ \mathbf{CG} \\ \mathbf{CG}^2 \\ \vdots \\ \mathbf{CG}^{N-2} \\ \mathbf{CG}^{N-1} \end{bmatrix},$$

$$\tilde{\mathbf{H}} = \begin{bmatrix} \mathbf{0} \\ \mathbf{CH} \\ \mathbf{C}(\mathbf{GH}+\mathbf{H}) \\ \vdots \\ \mathbf{C}\sum_{i=0}^{N-3}\mathbf{G}^i\mathbf{H} \\ \mathbf{C}\sum_{i=0}^{N-2}\mathbf{G}^i\mathbf{H} \end{bmatrix}, \mathbf{f}^*_k = \begin{bmatrix} \Delta f(k\tau) \\ \Delta f(k\tau+T) \\ \Delta f(k\tau+2T) \\ \vdots \\ \Delta f(k\tau+(N-3)T) \\ \Delta f(k\tau+(N-2)T) \end{bmatrix},$$

$$\mathbf{Q} = \begin{bmatrix} \mathbf{0} & \mathbf{0} & \cdots & \mathbf{0} & \mathbf{0} \\ \mathbf{CH} & \mathbf{0} & \cdots & \mathbf{0} & \mathbf{0} \\ \mathbf{CGH} & \mathbf{CH} & \cdots & \mathbf{0} & \mathbf{0} \\ \vdots & \vdots & \ddots & \vdots & \vdots \\ \mathbf{CG}^{N-3}\mathbf{H} & \mathbf{CG}^{N-4}\mathbf{H} & \cdots & \mathbf{CH} & \mathbf{0} \\ \mathbf{CG}^{N-2}\mathbf{H} & \mathbf{CG}^{N-3}\mathbf{H} & \cdots & \mathbf{CGH} & \mathbf{CH} \end{bmatrix}. \tag{15}$$

Since matrix $\tilde{\mathbf{G}}$ might not be invertible, instead of its regular inverse, Moore-Penrose matrix pseudoinverse, $\tilde{\mathbf{G}}^+$, is used to compute the estimated state. The pseudoinverse is calculated as [45]:

$$\tilde{\mathbf{G}}^+ = (\tilde{\mathbf{G}}^T\tilde{\mathbf{G}})^{-1}\tilde{\mathbf{G}}^T. \tag{16}$$

Although, if only equation (14) is used for state estimation, estimated values would be one sampling period delayed from the true values. Therefore, equation (14) is combined with the discrete-time approximation of system dynamics to obtain the estimated state as:

$$\hat{\mathbf{x}}_H((k+1)\tau) = \mathbf{G}_\tau\tilde{\mathbf{G}}^+(\mathbf{P}^*_{\mathbf{g}k} - \mathbf{Q}\mathbf{f}^*_k) + \mathbf{H}_\tau u(k\tau) + \mathbf{H}^\circ\mathbf{f}^*_k, \tag{17}$$

where is:

$$\mathbf{H}^\circ = \begin{bmatrix} \mathbf{G}^{N-1}\mathbf{H} & \mathbf{G}^{N-2}\mathbf{H} & \cdots & \mathbf{GH} & \mathbf{H} \end{bmatrix}, \tag{18}$$

while matrices $\mathbf{G}_\tau$ and $\mathbf{H}_\tau$ are obtained by ZOH discretization of the system from Fig. 7 (just like system (12), but with sampling period τ instead of T).

The results of the proposed state estimation method are shown in Fig. 9. Those results are obtained on the substitute linear model.

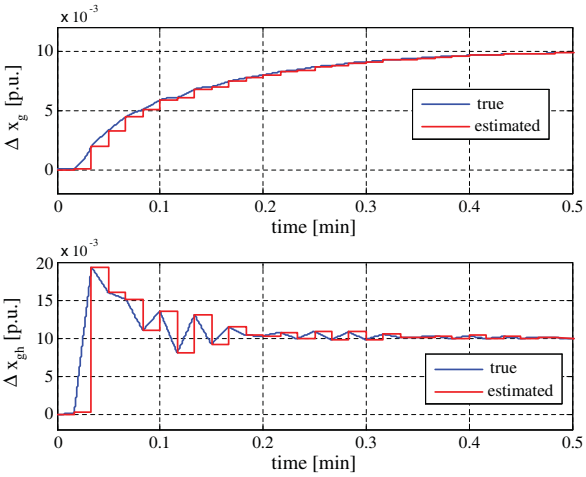

Fig. 9. Estimation of system state in CA1

From the figure it can be seen that FOS estimation gives very good results at sampling instants. Additionally, it can be seen that FOS estimation is independent of the chosen initial conditions, since the estimation error is very small, even in the first few seconds of the simulation.

4.2 Disturbance estimation

Total disturbance signal in CA1 consists of load disturbance, ΔP_{d1}, and the influence of neighbor CAs, e_1, which is:

$$e_1(t) = -\sum_{j=2}^{3}\left(K_{s1j}\Delta f_j(t)\right). \tag{19}$$

Total disturbance could also be estimated using FOS, but due to unknown disturbance dynamics the estimation would be τ seconds delayed [35]. Therefore, simpler and more accurate methods for disturbances estimation are presented here.

4.2.1 Load disturbance estimation

To estimate load disturbance two facts observed on the linear system model are utilized: 1) immediately after a step load disturbance occurs within a CA, the change in area's ACE signal is equal to the negative value of that disturbance; 2) after that load disturbance is compensated by LFC and ACE returned to zero, total change in power generated by power plants engaged in LFC is equal to the value of the disturbance. Therefore, the following equation can be used for load disturbance estimation:

$$\Delta\hat{P}_d(k\tau) = \Delta P_g(k\tau) - ACE(k\tau). \tag{20}$$

4.2.2 Estimation of the influence of neighbor CAs

A subsystem for estimating the influence of neighbor CAs is shown in Fig. 10.

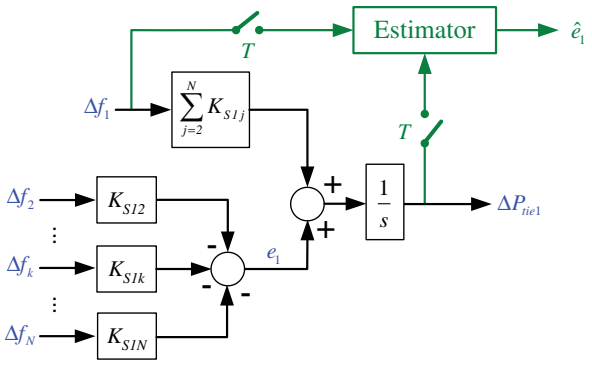

Fig. 10. A subsystem for estimating the influence of neighbor CAs to CA1

Since the influence of neighbor CAs to CA1 is simplified in the substitute model, it can be estimated by using discrete-time derivator:

$$\hat{e}_1(k\tau) = \frac{\Delta P_{tie1}(k\tau) - \Delta P_{tie1}((k-1)\tau)}{\tau} - \\ - \sum_{j=2}^{N} K_{s1j} \Delta f_1(k\tau). \tag{21}$$

Measurements of all signals needed to compute estimated values using (20) and (21) are available in the controller. Naturally, for model with uncertainties and for LFC application in real power system, those measurements must firstly be filtered through low pass filters to damp noise component and rapid changes in the signals.

The results of the proposed disturbance estimation methods are shown in Fig. 11. Those results are also obtained on the substitute linear model, with no uncertainties present in the model.

From the figure it can be seen that the disturbance estimations are slightly poorer than the state estimation, but still satisfactorily.

Altogether, estimation results from Figs. 9 and 11 show that the proposed methods can be used to estimate unmeasured state and disturbances in power system.

From the measurements and by using the proposed estimation equations (17), (20) and (21), full system state and disturbance of the substitute linear power system model are obtained. Therefore, a state based controller can now be designed for LFC. Since estimations are not perfect, they introduce estimation errors which can be observed as additional components of uncertainties $\boldsymbol{\xi}$ in (10). Therefore, a highly robust control algorithm is needed for LFC. That is the main reason why SMC is used for LFC in this paper.

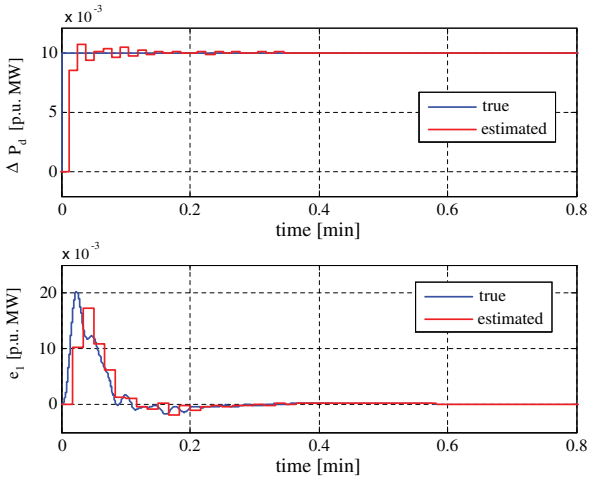

Fig. 11. Estimation of disturbances in CA1

5 DISCRETE-TIME SLIDING MODE CONTROL

SMC is a control technique appropriate for controlling time-variant systems in the presence of system uncertainties and external disturbances. If SMC based only on output signal is used for systems with non-minimum phase behavior, it will cause system instability [38]. Since hydro power plant is a system with non-minimum phase behavior, as it can be seen from Fig. 3, SMC based on full system state must be used for LFC in CA1.

To improve the overall system behavior, disturbance information is also included into controller's synthesis. Because all state and disturbances are not measurable, estimation techniques described in the previous section is used to obtain the values of their unmeasured components.

LFC based on SMC will be synthesized for discrete-time representation of system (10), where both disturbances (load disturbance and the influence of neighbor CAs) are gathered into one disturbance signal, $\mathbf{d}_t$, which results in the following system state equation:

$$\mathbf{x}((k+1)\tau) = \mathbf{G}_{ca}\mathbf{x}(k\tau) + \mathbf{H}_{ca}\mathbf{u}(k\tau) + \\ + \mathbf{W}_{ca}\mathbf{d}_t(k\tau) + \boldsymbol{\xi}_{ca}(\mathbf{x}, \mathbf{u}, k\tau). \tag{22}$$

For better insight into dynamics of system in sliding mode and for simpler controller synthesis it is more convenient to transform system (22) into a regular canonical form using transformation matrix $\mathbf{T}$ [38]:

$$\begin{bmatrix} \mathbf{x}_1((k+1)\tau) \\ \mathbf{x}_2((k+1)\tau) \end{bmatrix} = \begin{bmatrix} \mathbf{G}_{11} & \mathbf{G}_{12} \\ \mathbf{G}_{21} & \mathbf{G}_{22} \end{bmatrix} \begin{bmatrix} \mathbf{x}_1(k\tau) \\ \mathbf{x}_2(k\tau) \end{bmatrix} + \begin{bmatrix} \mathbf{0} \\ \mathbf{H}_2 \end{bmatrix} \mathbf{u}(k\tau) + \\ + \begin{bmatrix} \mathbf{W}_1 \\ \mathbf{W}_2 \end{bmatrix} \mathbf{d}_t(k\tau) + \begin{bmatrix} \boldsymbol{\xi}_u(\mathbf{x}, k\tau) \\ \boldsymbol{\xi}_m(\mathbf{x}, \mathbf{u}, k\tau) \end{bmatrix}, \tag{23}$$

where $\mathbf{x}_1$ and $\mathbf{x}_2$ represent state vectors of the decoupled subsystems of system (22), and it is $\begin{bmatrix}\mathbf{x}_1 & \mathbf{x}_2\end{bmatrix}^T = \mathbf{T}\mathbf{x}$. In the regular form, system's uncertainties are decoupled into matched ($\boldsymbol{\xi}_m$) and unmatched ($\boldsymbol{\xi}_u$) ones.

A sliding surface specifies system behavior in the sliding mode and it is defined as:

$$\boldsymbol{\sigma}(\mathbf{x}) \equiv \mathbf{S}\mathbf{x} = \mathbf{0}, \tag{24}$$

where $\mathbf{S} \in \mathbb{R}^{m\times n}$ is a switching matrix.

System (23) can be further transformed into [35]:

$$\begin{bmatrix}\mathbf{x}_1((k+1)\tau)\\ \boldsymbol{\sigma}((k+1)\tau)\end{bmatrix} = \begin{bmatrix}\hat{\mathbf{G}}_{11} & \hat{\mathbf{G}}_{12}\\ \hat{\mathbf{G}}_{21} & \hat{\mathbf{G}}_{22}\end{bmatrix}\begin{bmatrix}\mathbf{x}_1(k\tau)\\ \boldsymbol{\sigma}(k\tau)\end{bmatrix} + \begin{bmatrix}\mathbf{0}\\ \hat{\mathbf{H}}_2\end{bmatrix}\mathbf{u}(k\tau) + \\ + \begin{bmatrix}\mathbf{W}_1\\ \hat{\mathbf{W}}_2\end{bmatrix}\mathbf{d}(k\tau) + \begin{bmatrix}\boldsymbol{\xi}_u(\mathbf{x},k\tau)\\ \boldsymbol{\xi}_s(\mathbf{x},\mathbf{u},k\tau)\end{bmatrix}, \tag{25}$$

where are:

$$\begin{aligned}&\begin{bmatrix}\mathbf{S}_1 & \mathbf{S}_2\end{bmatrix} = \mathbf{S}\mathbf{T}^{-1},\\ &\hat{\mathbf{G}}_{11} = \mathbf{G}_{11} - \mathbf{G}_{12}\mathbf{S}_2^{-1}\mathbf{S}_1,\\ &\hat{\mathbf{G}}_{12} = \mathbf{G}_{12}\mathbf{S}_2^{-1},\\ &\hat{\mathbf{G}}_{21} = \mathbf{S}_1(\mathbf{G}_{11} - \mathbf{G}_{12}\mathbf{S}_2^{-1}\mathbf{S}_1) + \mathbf{S}_2(\mathbf{G}_{21} - \mathbf{G}_{22}\mathbf{S}_2^{-1}\mathbf{S}_1),\\ &\hat{\mathbf{G}}_{22} = \mathbf{S}_1\mathbf{G}_{12}\mathbf{S}_2^{-1} + \mathbf{S}_2\mathbf{G}_{22}\mathbf{S}_2^{-1},\\ &\hat{\mathbf{H}}_2 = \mathbf{S}_2\mathbf{H}_2,\\ &\hat{\mathbf{W}}_2 = \mathbf{S}_1\mathbf{W}_1 + \mathbf{S}_2\mathbf{W}_2,\\ &\boldsymbol{\xi}_s(\mathbf{x},\mathbf{u},k\tau) = \mathbf{S}_1\boldsymbol{\xi}_u(\mathbf{x},k\tau) + \mathbf{S}_2\boldsymbol{\xi}_m(\mathbf{x},\mathbf{u},k\tau).\end{aligned} \tag{26}$$

As it can be seen from (25), when the system is in the sliding mode ($\boldsymbol{\sigma}(k\tau) = \mathbf{0}$), matched uncertainties do not influence the system's dynamics. Therefore, SMC is robust to matched uncertainties, although only at the sampling instants, since between them the system is not in the sliding mode.

The control law that ensures sliding mode will be computed according to (25), by an appropriate choice of a reaching law. The reaching law is in charge of driving system's trajectory to the sliding surface. Among several known reaching laws [46–50], a linear reaching law from [50] is chosen to be used for LFC, because it exactly defines the trajectory towards the sliding surface and its usage results in straightforward controller design [38]. It is defined as:

$$\boldsymbol{\sigma}((k+1)\tau) = \boldsymbol{\Lambda}\boldsymbol{\sigma}(k\tau), \tag{27}$$

where $\boldsymbol{\Lambda}$ is a diagonal matrix whose elements are constrained to $0 \leq \lambda_i < 1$.

If reaching law (27) is applied to system (25) and uncertainties neglected, the following control law is obtained:

$$\mathbf{u}(k\tau) = \hat{\mathbf{H}}_2^{-1}\left[(\boldsymbol{\Lambda} - \hat{\mathbf{G}}_{22})\boldsymbol{\sigma}(k\tau) - \right. \\ \left. - \hat{\mathbf{G}}_{21}\mathbf{x}_1(k\tau) - \hat{\mathbf{W}}_2\mathbf{d}(k\tau)\right]. \tag{28}$$

The control law (28) will ensure that system trajectory resides in a narrow band around the sliding surface. The width of that band primarily depends on the maximal value of uncertainties and upon the value of matrix $\boldsymbol{\Lambda}$ from (27). To reduce its width, uncertainties are also estimated.

5.1 Uncertainties estimation

Generally, uncertainties in systems are mostly composed of noise, unmodeled system dynamics and time variations of system parameters. Additionally, the proposed controller synthesis introduces a few additional components of system uncertainties which are caused by identification, linearization and estimation errors.

Uncertainties estimation is obtained from the difference of true and the ideal system behavior in sliding mode. Therefore, the estimated uncertainties are computed as [38]:

$$\hat{\boldsymbol{\xi}}_s(k\tau) = \hat{\boldsymbol{\xi}}_s((k-1)\tau) + \boldsymbol{\sigma}(k\tau) - \boldsymbol{\Lambda}\boldsymbol{\sigma}((k-1)\tau). \tag{29}$$

If estimated uncertainties from (29) are included into control law (28), the following control law is obtained:

$$\mathbf{u}(k\tau) = \hat{\mathbf{H}}_2^{-1}\left[(\boldsymbol{\Lambda} - \hat{\mathbf{G}}_{22})\boldsymbol{\sigma}(k\tau) - \hat{\mathbf{G}}_{21}\mathbf{x}_1(k\tau) - \right. \\ \left. - \hat{\mathbf{W}}_2\mathbf{d}(k\tau) - \hat{\boldsymbol{\xi}}_s(k\tau)\right]. \tag{30}$$

With control law (30), the width of the band around the sliding surface becomes dependent on the maximal rate of change of uncertainties, instead on their maximal value [38]. For uncertainties present in power system, that would result in reduction of width of the band around the sliding surface.

In this section, discrete-time SMC was derived for a general minimum-phase system. In the next section it will be applied to LFC system.

6 LOAD-FREQUENCY CONTROL BASED ON DISCRETE-TIME SLIDING MODE CONTROL

If discrete-time SMC is applied in LFC controller, there will be only one sliding surface, since the control signal in LFC has dimension one ($m = 1$, $\mathbf{u} \equiv u$). Furthermore, switching matrix becomes a switching vector and reaching law matrix becomes a scalar ($\boldsymbol{\Lambda} \equiv \lambda$).

According to state vector from (2), a switching vector for CA1 is:

$$\mathbf{S} = \begin{bmatrix}s_f & s_{Ptie} & s_{Pg} & s_{xg} & s_{xgh}\end{bmatrix}. \tag{31}$$

Additionally, according to (25), system's stability in sliding mode is ensured if the parameters of the switching

vector are chosen such that matrix $\hat{\mathbf{G}}_{11}$ has all its eigenvalues within the unit circle.

Discrete-time SMC ensures that system trajectory only resides in a narrow band around the sliding surface, but unfortunately that doesn't imply zero value of ACE in steady state [35], which is inherent to PI controller. Therefore, in order to ensure system stability and to minimize zero steady-state error of ACE, an appropriate relation between the parameters of the switching vector must be found. In [35] it is shown that with uncertainties neglected, steady state ACE will be equal to zero if the following conditions are satisfied:

$$\begin{aligned} s_{Pg} + s_{xg} + s_{xgh} &= 0, \\ s_{Ptie} &\neq 0. \end{aligned} \tag{32}$$

Furthermore, since system behavior in SMC doesn't change if the switching vector is multiplied by any non-zero scalar, it can be set $s_{Pg} = 1$.

Altogether, SMC controller synthesis reduces down to finding optimal values of parameters λ, s_f, s_{Ptie} and s_{xg}. Again, an appropriate GA is used as search algorithm for that purpose.

6.1 Optimal sliding mode control algorithm parameters

In controller synthesis, GA is used to find optimal values of the following set of controller's independent parameters:

$$\boldsymbol{\Theta} = \begin{bmatrix} s_f & s_{Ptie} & s_{xg} & \lambda \end{bmatrix}. \tag{33}$$

GA used for finding optimal controller parameters is similar to GA used for substitute linear model identification in Section 3. However its flow chart is slightly different from the flow chart shown in Fig. 4. The first difference is that the flow chart for controller synthesis has additional block for computing the control law (30), which is placed just above block *Simulation* in Fig. 4 [37].

The other difference is that the fitness function for controller synthesis purposes is given as:

$$\Phi_c(\boldsymbol{\Theta}) = \int_0^{T_s} (ACE(t))^2 \cdot z(t)dt + \mu\,(u(t))^2\,dt, \tag{34}$$

where $\boldsymbol{\Theta}$ is given in (33), μ is a weighting factor and z is a weighting ramp function which reduces the influence of variations in ACE in the first moments after the disturbance.

Parameters of the GA used for controller synthesis are shown in Tab. 3.

By using the proposed GA, the optimal controller parameters in CA1 are obtained as: $\lambda = 0.990$ and $\mathbf{S} = \begin{bmatrix} -74 & -0.057 & 1 & -98.096 & 97.096 \end{bmatrix}$.

Table 3. Parameters of GA used for controller synthesis

Parameter	Description	Value
r	Size of population	100
g	Genes per chromosome	7
b	Bits per gene	15
p_c	Probability of crossover	0.7
p_m	Probability of mutation	0.05
N_g	Number of generations	200
μ	Input signal weighting factor	0.01

Altogether, the complete scheme of the proposed LFC algorithm is shown in Fig. 12. The procedure starts from nonlinear power system model and uses GA and recorded measured signals from that model to identify parameters of the substitute linear system model. If the proposed algorithm is to be installed in real power system, the used signals from the nonlinear model should be replaced with true measured signals.

Continuous-time SMC is applied to continuous-time system model resulting in steady state accuracy condition, given by (32). Discrete-time SMC is then applied to discrete-time system model to obtain control law (30). By simulations on continuous-time model and by using the accuracy condition and the proposed control law, GA is used to find the optimal controller parameters. All above-mentioned steps of the algorithm are done off-line, and they are based on measurement data, recorded through certain time period.

The only on-line computations are performed within two blocks inside Load frequency controller in Fig. 12.

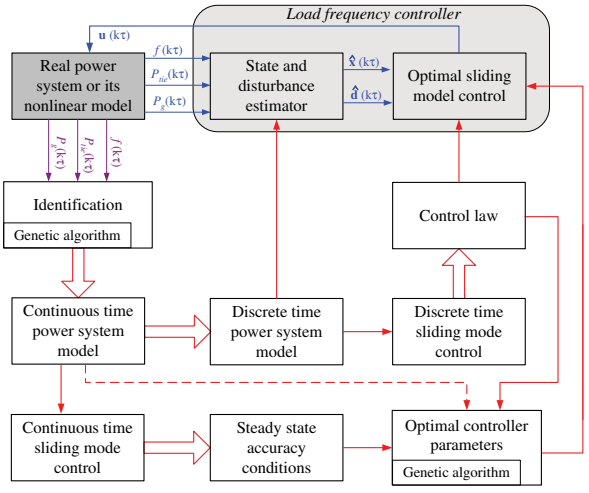

Fig. 12. An algorithm scheme of LFC based on discrete-time SMC

Firstly, measured signals and discrete-time system model are used to estimate unmeasured power system state and disturbances. Secondly, sliding mode controller (with previously off-line calculated optimal parameters) is used to compute the control signal, which is then distributed among power plants engaged in LFC [51].

7 SIMULATION RESULTS ON NONLINEAR POWER SYSTEM MODEL

In the simulations, the proposed algorithm is used for LFC in CA1 from Fig. 2, while in all other CAs common PI controllers are used. PI controllers are also derived in discrete time with parameters obtained using GA in order to minimize fitness function (34).

In the simulations, the sample times are set to $\tau = 1$ s and $T = 0.2$ s.

Several disturbances occur during the simulation: 1) multiple switching on/off of portions of load in CA1 (Load 1A, Load 2A, Load 3A and Load 3B in Fig. 2), 2) turning off of a power plant in CA1 which is not engaged in LFC (TPP 2 in Fig. 2), 3) single switching on/off of portions of loads in neighbor CAs, 4) changing generation schedule of a power plant in CA1 not engaged in LFC and 5) changing exchange schedule between areas CA1 and CA2.

All the disturbances in CA1 are shown in Fig. 13. The first plot of Fig. 13 shows total load (P_L) in CA1, measured during the simulation. The second plot shows generation schedules (P_{ref}) of power plants in CA1 that are not engaged in LFC. It can be seen that power plant TPP 2 shuts down after 20 minutes and power plant TPP 1 changes its generation schedule. The third plot shows exchange schedule between CA1 and CA2 (P_{12}). Generation and exchange schedules are carried out using ramps, which is common in real power systems [43].

Unlike small disturbances used for controller validation on linear power system models [3,11,14,26,30], some disturbances from Fig. 13 are significantly large, especially those regarding turning off substantial load component at $t = 4$ min (seen on the first plot of Fig. 13) or turning off the entire power plant at $t = 20$ min (seen on the second plot of Fig. 13).

ACE signal in CA1 is shown in Fig. 14 and the switching function in CA1 is shown in Fig. 15. It can be seen from Fig. 14 that the proposed controller compensates for every disturbance in the system by returning ACE signal in the vicinity of zero after each disturbance. The dynamics of the compensations are similar for different disturbances, since they are determined by the chosen controller parameters. Besides, only large disturbances cause considerable system's deviation from sliding mode, but the return to the vicinity of the surface is very fast, as it can be seen from Fig. 15.

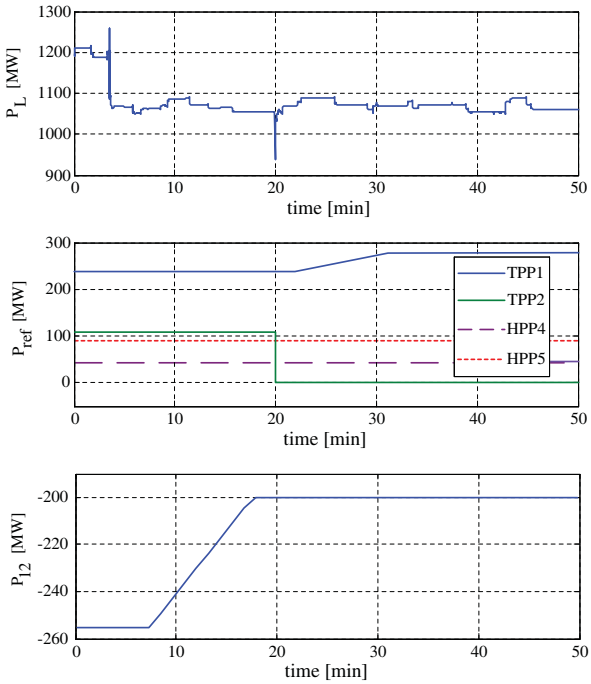

Fig. 13. Disturbances in CA1: P_L - load, P_{ref} - planned generation of power plants not engaged in LFC, and P_{12} - planned exchange with CA2

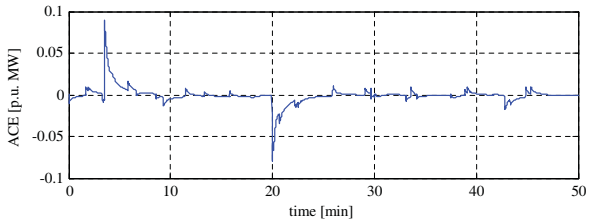

Fig. 14. ACE signal in CA1

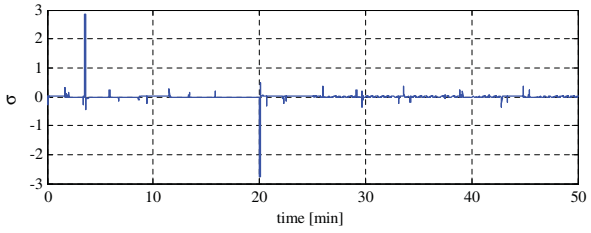

Fig. 15. Switching function in CA1

In Fig. 16 the total control signal of the proposed controller and output active powers of power plants engaged in LFC are shown. Total control signal is divided among

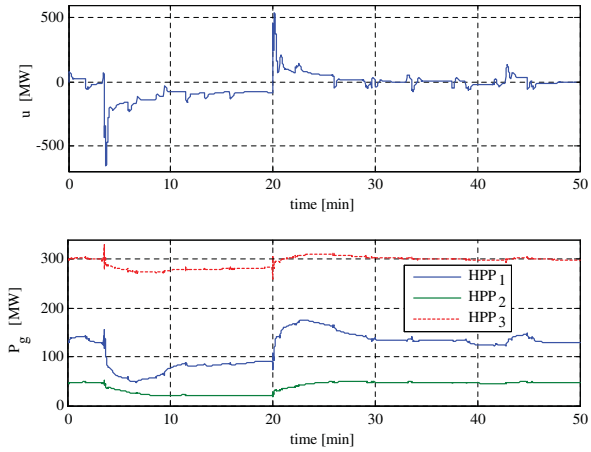

Fig. 16. Total LFC control signal and output active powers of power plants engaged in LFC in CA1

the plants engaged in LFC, depending on their participation factors. The participation factors are set to $\kappa_1 = 0.5$, $\kappa_2 = 0.3$ and $\kappa_3 = 0.2$. It can be seen from the figure that HPP 1 takes over the largest share in change of generation, since it has the largest participation factor. Static participation factors are used here for simplicity and their dynamic calculation and optimization is addressed in [51].

A comparison between PI controller and the proposed controller is not addressed here, since in [35] and [37] it has already been shown that the proposed controller outperforms classical PI controller.

8 CONCLUSIONS

In this paper a discrete-time sliding mode based load-frequency controller is designed based on nonlinear power system model. The controller is designed for power systems with only hydro power plants engaged in LFC, since those types of models are not sufficiently treated in available LFC studies. Since sliding mode controller for non-minimum phase system needs full-state feedback, all unmeasured system states and disturbances are estimated using FOS. The standard FOS estimation method has been slightly modified so it could also be used for disturbance estimation. GAs are used for finding optimal parameters of the substitute linear model and SMC controller.

The proposed controller is validated through simulations on power system model consisting of four different control areas. Simulation results show very good compensation of various disturbances in the system. Because good behavior of the proposed controller is hereby confirmed on detailed nonlinear power system model, there are no obstacles to keep further development of the algorithm and eventually implement it in real power system.

ACKNOWLEDGEMENTS

This work has been financially supported by The National Foundation for Science, Higher Education and Technological Development of the Republic of Croatia and Končar - Power Plant and Electric Traction Engineering, Zagreb, Croatia.

REFERENCES

[1] ENTSO-E. http://www.entsoe.eu.

[2] A. Germond and R. Podmore, "Dynamic aggregation of generating unit models," *IEEE Transactions on Power Apparatus and Systems*, vol. PAS-97, no. 4, pp. 1060–1069, 1978.

[3] S. Velusami and I. Chidambaram, "Decentralized biased dual mode controllers for load frequency control of interconnected power systems considering GDB and GRC nonlinearities," *Energy Conversion and Management*, vol. 48, no. 5, pp. 1691–1702, 2007.

[4] Q. Ha, "A fuzzy sliding mode controller for power system load-frequency control," in *Second International Conference on Knowledge-Based Intelligent Electronic Systems, Adelaide, South Australia*, pp. 149–154, 1998.

[5] H. Zeynelgil, A. Demiroren, and N. Sengor, "The application of ANN technique to automatic generation control for multi-area power system," *International Journal of Electrical Power & Energy Systems*, vol. 24, no. 5, pp. 345–354, 2002.

[6] K. Yamashita and T. Taniguchi, "Optimal observer design for load-frequency control," *International Journal of Electrical Power & Energy Systems*, vol. 8, no. 2, pp. 93–100, 1986.

[7] S. Tripathy, R. Balasubramanian, and P. C. Nair, "Small rating capacitive energy storage for dynamic performance improvement of automatic generation control," *Generation, Transmission and Distribution IEE Proceedings C*, vol. 138, no. 1, pp. 103–111, 1991.

[8] Y. Karnavas and D. Papadopoulos, "AGC for autonomous power system using combined intelligent techniques," *Electric Power Systems Research*, vol. 62, no. 3, pp. 225–239, 2002.

[9] T. Inoue and A. Amano, "A thermal power plant model for dynamic simulation of load frequency control," in *IEEE PES Power Systems Conference & Exposition*, pp. 1442–1447, 2006.

[10] K. Divya and P. S. N. Rao, "A simulation model for AGC studies of hydro–hydro systems," *International Journal of Electrical Power & Energy Systems*, vol. 27, no. 5-6, pp. 353–342, 2005.

[11] A. Khodabakhshian and N. Golbon, "Robust load frequency controller design for hydro power systems," in *Proceedings of the 2005 IEEE Conference on Control Applications, Toronto, Canada*, pp. 1510–1515, 2005.

[12] E. Cam, "Application of fuzzy logic for load frequency control of hydroelectrical power plants," *Energy Conversion and Management*, vol. 48, no. 4, pp. 1281–1288, 2007.

[13] S. Doolla and T. Bhatti, "Automatic generation control of an isolated small-hydro power plant," *Electric Power Systems Research*, vol. 76, no. 9-10, pp. 889–896, 2006.

[14] H. Bevrani and T. Hiyama, "Robust decentralised PI based LFC design for time delay power systems," *Energy Conversion and Management*, vol. 49, no. 2, pp. 193–204, 2008.

[15] D. Iracleous and A. Alexandridis, "A multi-task automatic generation control for power regulation," *Electric Power Systems Research*, vol. 73, no. 3, pp. 275–285, 2005.

[16] Y. Rebours, D. Kirschen, M. Trotignon, and S. Rossignol, "A survey of frequency and voltage control ancillary services-part I: Technical features," *IEEE Transactions on Power Systems*, vol. 22, no. 1, pp. 350–357, 2007.

[17] B. Stojković, "An original approach for load-frequency control - the winning solution in the second UCTE synchronous zone," *Electric Power Systems Research*, vol. 69, no. 1, pp. 59–68, 2004.

[18] N. Al-Musabi, "Design of optimal variable structure controllers: Applications to power system dynamics," Master's thesis, King Fahd University of Petroleum and Minerals, Dhahran, Saudi Arabia, 2004.

[19] J. Frunt, A. Jokic, W. Kling, J. Myrzik, and P. van den Bosch, "Provision of ancillary services for balance management in autonomous networks," in *5th International Conference on European Electricity Market, EEM 2008*, pp. 1–6, 2008.

[20] B. Fardanesh, "Future trends in power system control," *IEEE Computer Applications in Power*, vol. 15, no. 3, pp. 24–31, 2002.

[21] Ibraheem, P. Kumar, and D. Kothari, "Recent philosophies of automatic generation control strategies in power systems," *IEEE Transactions on Power Systems*, vol. 20, no. 1, pp. 246–357, 2005.

[22] H. Shayeghi, H. Shayanfar, and A. Jalili, "Load frequency control strategies: A state-of-the-art survey for the researcher," *Energy Conversion and Management*, vol. 50, no. 2, pp. 344–353, 2008.

[23] W. Tan and Z. Xu, "Robust analysis and design of load frequency controller for power systems," *Electric Power Systems Research*, vol. 79, no. 5, pp. 846–853, 2009.

[24] H. Lee, J. Park, and Y. Joo, "Robust load-frequency control for uncertain nonlinear power systems: A fuzzy logic approach," *Information Sciences*, vol. 176, no. 23, pp. 3520–3537, 2006.

[25] A. Hemeida, "Wavelet neural network load frequency controller," *Energy Conversion and Management*, vol. 46, no. 9-10, pp. 1613–1630, 2005.

[26] H. Shayeghi and H. Shayanfar, "Application of ANN technique based on μ-synthesis to load frequency control of interconnected power system," *International Journal of Electrical Power & Energy Systems*, vol. 28, no. 7, pp. 503–511, 2006.

[27] N. Atić, A. Feliachi, and D. Rerkpreedapong, "CPS1 and CPS2 compliant wedge-shaped model predictive load frequency control," in *2004 IEEE Power Engineering Society General Meeting*, pp. 855–860, 2004.

[28] A. Venkat, I. Hiskens, J. Rawlings, and S. Wright, "Distributed output feedback MPC for power system control," in *45th IEEE Conference on Decision and Control, San Diego, USA*, pp. 4038–4045, 2006.

[29] A. Demiroren and H. Zeynelgil, "GA application to optimization of AGC in three-area power system after deregulation," *International Journal of Electrical Power & Energy Systems*, vol. 29, no. 3, pp. 230–240, 2007.

[30] C. Parisses, N. Asimopoulos, and P. Fessas, "Decentralized load-frequency control of a two-area power system via linear programming and optimization techniques," in *Proceedings of 5th International Conference on Technology and Automation, Thessaloniki, Greece*, pp. 204–209, 2005.

[31] S. Hosseini and A. Etemadi, "Adaptive term neuro-fuzzy inference system based automatic generation control," *Electric Power Systems Research*, vol. 78, no. 7, pp. 1230–1239, 2008.

[32] M. Zribi, M. Al-Rashed, and M. Alrifai, "Adaptive decentralized load frequency control of multi-area power systems," *International Journal of Electrical Power & Energy Systems*, vol. 27, no. 8, pp. 575–583, 2005.

[33] Y. Hsu and W. Chan, "Optimal variable structure controller for the load-frequency control of interconnected hydrothermal power systems," *International Journal of Electrical Power & Energy Systems*, vol. 6, no. 4, pp. 221–229, 1984.

[34] F. Okafor, "Variable structure unit vector control of electric power generation," *African Journal of Science and Technology - Science and Engineering Series*, vol. 1, no. 4, pp. 78–86, 2001.

[35] K. Vrdoljak, N. Perić, and I. Petrović, "Sliding mode based load frequency control in power systems," *Electric Power Systems Research*, vol. 80, no. 5, pp. 514–527, 2010.

[36] SimPowerSystems. http://www.mathworks.com/products/simpower.

[37] K. Vrdoljak, *Sliding Mode Based Load Frequency Control in Power Systems*. PhD thesis, Faculty of Electrical Engineering and Computing, University of Zagreb, 2009. In Croatian.

[38] G. Monsees, *Discrete-Time Sliding Mode Control*. PhD thesis, Delft University of Technology, Netherlands, 2002.

[39] B. Horvat and A. Černicki Mijić, "Reconnecting of the HPP Senj in load frequency control system of the Croatian EPS using new technologies," in *7th HO CIGRE Session, Cavtat, Croatia*, pp. 1320–1330, 2005. In Croatian.

[40] M. Saaj, B. Bandyopadhyay, and H. Unbehauen, "A new algorithm for discrete-time sliding-mode control using fast output sampling feedback," *IEEE Transactions on Industrial Electronics*, vol. 49, no. 3, pp. 518–523, 2002.

[41] K. Vrdoljak, T. Radošević, and N. Perić, "Identification of power system model parameters for sliding mode based load-frequency control," in *Proceedings of the International IEEE Conference EUROCON 2009, St. Petersburg, Russia*, pp. 540–547, 2009.

[42] P. Fleming and R. Purshouse, "Evolutionary algorithms in control systems engineering: a survey," *Control Engineering Practice*, vol. 10, no. 11, pp. 1223–1241, 2002.

[43] UCTE, "Operational handbook - load-frequency control and performance," 2004. http://www.ucte.org.

[44] S. Janardhanan, *Multirate Output Feedback based Discrete-time Sliding Mode Control Strategies*. PhD thesis, Indian Institute of Technology, Bombay, India, 2005.

[45] A. Ben-Israel and T. Greville, *Generalized Inverses*. Springer-Verlag, 2003.

[46] S. Sarpturk, Y. Istefanopulos, and O. Kaynak, "On the stability of discrete time sliding mode control systems," *IEEE Transactions on Automatic Control*, vol. 32, no. 10, pp. 930–932, 1987.

[47] K. Furuta, "Sliding mode control of discrete system," *System & Control Letters*, vol. 14, no. 2, pp. 145–152, 1990.

[48] W. Gao, Y. Wang, and A. Homaifa, "Discrete time variable structure control systems," *IEEE Transactions on Industrial Electronics*, vol. 42, no. 2, pp. 117–122, 1995.

[49] A. Bartoszewicz, "Discrete-time quasi-sliding mode control strategies," *IEEE Transactions on Industrial Electronics*, vol. 45, no. 4, pp. 633–637, 1998.

[50] S. Spurgeon, "Hyperplane design techniques for discrete-time variable structure control systems," *International Journal on Control*, vol. 55, no. 2, pp. 445–456, 1992.

[51] K. Vrdoljak, N. Perić, and D. Šepac, "Optimal distribution of load-frequency control signal to hydro power plants," in *Proceedings of 2010 IEEE International Symposium on Industrial Electronics (ISIE)*, 2010.

Krešimir Vrdoljak received his B.Sc. and Ph.D. degrees in Electrical Engineering from the University of Zagreb, Croatia in 2003 and 2009, respectively. From 2003 to 2009 he was employed at the Department of Control and Computer Engineering at the Faculty of Electrical Engineering and Computing in Zagreb, Croatia. He is currently employed at Končar - Power Plant and Traction Engineering Inc., Zagreb, Croatia. His research interests are in advanced control techniques applied to power systems.

Nedjeljko Perić (1950.) has been professionally working for the last thirty five years as a scientist and researcher in the area of automatic control and automation of complex processes and systems. His scientific and professional work can be grouped into two distinct phases. During the first phase he was working at the Končar's Institute of Electrical Engineering (1973-1993) with emphasis on development of the automation systems for complex processes. In particular, he initiated and led the corporate research and development programs for the microprocessor control of electrical machines and related fast processes. The second phase of his work is connected to the employment at the Faculty of Electrical Engineering and Computing in Zagreb (from 1993 onwards), where he has initiated a broad research activity in advanced control of complex and large scale technical systems. His research results are published in scientific journals (more than 30 papers), proceedings of international conferences (more than 200 papers), and in numerous research studies/reports (more than 60 reports). Prof. Perić has particularly excelled in the leadership of national and international research projects. For his work he has received numerous awards, among others, the Croatian national award for science (for year 2007) for important scientific achievement in development of advanced control and estimation strategies for complex technical systems. He has also received the "Fran Bošnjaković" award (in 2009) for the exceptional contribution to the development and promotion of the automatic control research field within the area of technical sciences.

Ivan Petrović received B.Sc. degree in 1983, M.Sc. degree in 1989 and Ph.D. degree in 1998, all in Electrical Engineering from the Faculty of Electrical Engineering and Computing (FER Zagreb), University of Zagreb, Croatia. He had been employed as an R&D engineer at the Institute of Electrical Engineering of the Končar Corporation in Zagreb from 1985 to 1994. Since 1994 he has been with FER Zagreb, where he is currently the head of the Department of Control and Computer Engineering. He teaches a number of undergraduate and graduate courses in the field of control systems and mobile robotics. His research interests include various advanced control strategies and their applications to control of complex systems and mobile robots navigation. Results of his research effort have been implemented in several industrial products. He is a member of IEEE, IFAC - TC on Robotics and FIRA - Executive committee. He is a collaborating member of the Croatian Academy of Engineering.

AUTHORS' ADDRESSES

Krešimir Vrdoljak, Ph.D.
KONČAR - Power Plant and Traction Engineering Inc.,
Fallerovo šetalište 22, HR-10000 Zagreb, Croatia,
email: kresimir.vrdoljak@koncar-ket.hr

Prof. Nedjeljko Perić, Ph.D.
Prof. Ivan Petrović, Ph.D.
Department of Control and Computer Engineering,
Faculty of Electrical Engineering and Computing,
University of Zagreb,
Unska 3, HR-10000 Zagreb, Croatia
emails: nedjeljko.peric@fer.hr, ivan.petrovic@fer.hr

Received: 2009-12-04
Accepted: 2010-02-11